

Self-Assembly of Zinc Porphyrins around the Periphery of Hydrogen-Bonded Aggregates That Bear Imidazole Groups

Eric E. Simanek, Lyle Isaacs, Xinhua Li, Clay C. C. Wang, and George M. Whitesides*

Department of Chemistry and Chemical Biology, Harvard University, 12 Oxford Street, Cambridge, Massachusetts 02138




Received August 8, 1996[®]

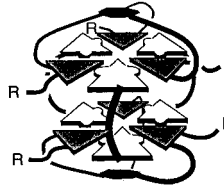
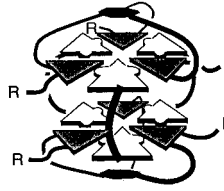
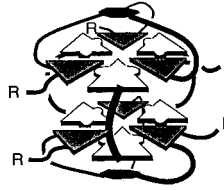
This paper describes the preparation and characterization of four aggregates that are based on the rosette of derivatives of isocyanuric acid (CA) and melamine (M). These aggregates comprise a trismelamine, $\text{hub}(\text{M}^{\text{Im}})_3$, that presents imidazole groups around its periphery; these imidazoles organize zinc tetraphenyl porphyrin (ZnTPP) by coordination of the imidazole to the zinc center. Aggregate **1** forms a single rosette upon mixing 1 equiv of $\text{hub}(\text{M}^{\text{Im}})_3$ and 3 equiv of CA. Adding 3 equiv of ZnTPP yields **2**. Aggregate **3** forms as a stacked bisrosette upon mixing 2 equiv of $\text{hub}(\text{M}^{\text{Im}})_3$ and 3 equiv of bisCA. Adding 6 equiv of ZnTPP yields **4**. The stoichiometries of aggregates **1–4** were obtained by titrating the trismelamines with CA and by titrating the aggregates with ZnTPP. The stoichiometry is defined as the ratio at which additional CA remains insoluble or additional ZnTPP appears as free ZnTPP in the ^1H NMR spectrum. Electrospray ionization mass spectrometry (ESI-MS) is compatible with the measured stoichiometries. The structures of these aggregates were determined using variable-temperature ^1H NMR spectroscopy; analogous structures were inferred for **5** and **6**, the *tert*-butyl analogues of **1** and **2**. The shapes of the traces from gel permeation chromatography (GPC) suggest that imidazole groups destabilize the aggregates when they are not involved in coordination to zinc; that is, the stability seems to be $6 \approx 4 > 3$ and $5 \approx 2 > 1$. A direct comparison of the relative stability of **1**, **2**, and **5** confirms the results of the GPC analysis: mixing **1** ($\text{hub}(\text{M}^{\text{Im}})_3 \cdot 3\text{CA}$) with the trismelamine component of **5** ($\text{hub}(\text{M})_3$) leads to the formation of a 3:2 mixture of **5:1**. Adding ZnTPP to this solution leads to a 3:2 mixture of **5:2** with free trismelamines remaining in solution: **1** is not observed. The results of UV/vis spectroscopy are consistent with the other spectroscopic and chromatographic results and indicate that 3 equiv of ZnTPP are organized around the periphery of **2** and at least 4 equiv around the periphery of **4**.

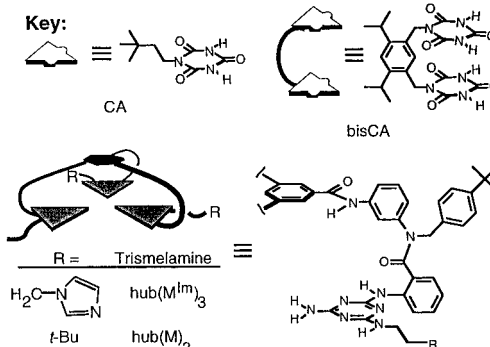
Introduction

This paper describes research that is part of a program whose objectives include the construction of large, soluble aggregates from simple precursors using molecular self-assembly. This program has focused on a family of aggregates based on the hydrogen-bonded lattice formed from isocyanuric acid and melamine (CA·M).¹ Our choice of CA·M reflects the necessity for (i) large numbers of hydrogen bonds to provide a large enthalpy of formation and balance the large, unfavorable entropy of formation, (ii) molecules with easily functionalized sites, and (iii) a structure for the aggregate that is highly symmetric to simplify characterization. Aggregates **5** and **6** (Table 1) are representative of early efforts. Here, we report the incorporation of zinc tetraphenyl porphyrin-imidazole interactions into derivatives of **5** and **6**.

There are four advantages to using zinc-imidazole interactions in addition to hydrogen bonds to generate aggregates of high molecular weight. First, zinc porphyrin-imidazole interactions are strong (approximately 8 kcal mol⁻¹).⁴ Second, zinc-imidazole interactions do not interfere with the hydrogen-bond interac-

Aggregate	R	ZnTPP (equiv)
	Im	0
	Im	3
	<i>t</i> -Bu	0

	Im	0
	Im	6
	<i>t</i> -Bu	0



tions that provide the major structural elements forming the central rosette. Third, zinc-imidazole interactions can be incorporated into aggregates based on CA·M on

[®] Abstract published in *Advance ACS Abstracts*, December 1, 1997.

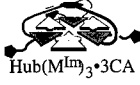

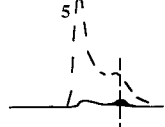
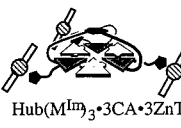
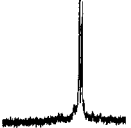
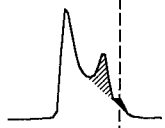

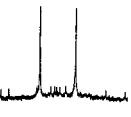
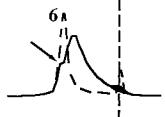
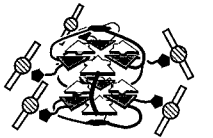
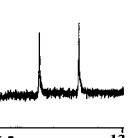

(1) Whitesides, G. M.; Simanek, E. E.; Mathias, J. P.; Seto, C. T.; Chin, D. N.; Mammen, M.; Gordon, D. M. *Acc. Chem. Res.* **1995**, *27*, 37.

(2) Seto, C. T.; Mathias, J. P.; Whitesides, G. M. *J. Am. Chem. Soc.* **1993**, *115*, 1321.

(3) Chin, D. N.; Gordon, D. M.; Whitesides, G. M. *J. Am. Chem. Soc.* **1994**, *116*, 12033. Chin, D. N.; Simanek, E. E.; Li, X.; Wazeer, M. I. M.; Whitesides, G. M. *J. Org. Chem.* **1997**, *62*, 1891.

(4) Kadish, K. M.; Shiue, L. R.; Rhodes, R. K.; Bottomley, L. A. *Inorg. Chem.* **1981**, *20*, 1274. Mashiko, T.; Dolphin, D. in *Comprehensive Coordination Chemistry*; Wilkinson, G., Gillard, R. D., McCleverty, J. A., Eds.; Pergamon Press: New York, 1987; Vol. 2, pp 813–898.

Table 2. Summary of the Characterization of 1–4^a

Aggregate:	ESI-MS		Imide region:	GPC:
	Ion:	Other Ions:		
 Hub(M ^{Im}) ₃ •3CA	1	1•Cl ⁻ NONE		
 Hub(M ^{Im}) ₃ •3CA•3ZnTPP	2	2•2Cl ⁻ 2•2Cl ⁻ - ZnTPP 2•2Cl ⁻ - 2ZnTPP		
 2Hub(M ^{Im}) ₃ •3bisCA	3	3•2Cl ⁻ NONE		
 2Hub(M ^{Im}) ₃ •3bisCA•6ZnTPP	4	4•3Cl ⁻ 4•3Cl ⁻ + ZnTPP 4•3Cl ⁻ + ZnTPP - CA 4•3Cl ⁻ - CA		

^a "Aggregate" is defined in Table 1. "Ion" refers to the stoichiometry of the line observed in ESI-MS. "Others" lists other major lines seen in the mass spectrogram. The "imide region" of the NMR spectra refers to the region between 16.5 and 13.5; the scale of **3** is offset by 0.5 ppm. The traces obtained by "GPC" are shown. The dashed traces (corresponding to **5** and **6**) are included so that comparisons of **5** with **1** and **6** with **3** can be made efficiently. These dashed traces were collected separately and do not represent the result of coinjection of aggregates. The hatched area corresponds to free ZnTPP. The shaded area is a molecular weight standard (*p*-xylene). An arrow is used to identify the sharp leading edge of **3**.

the periphery of the central rosette so that established strategies for characterization can be used. Fourth, working with zinc-imidazole interactions allows us to take advantage of a wealth of literature on self-assembly based on the coordination chemistry of porphyrins.^{4–6}

The goals of this work were to determine (i) the effect of the imidazole group on the stability of hydrogen-bonded aggregates in the absence of metal-containing groups and (ii) the ability of the imidazole groups to form stable zinc-imidazole interactions. We use zinc tetraphenylporphyrin (ZnTPP) as a coordinating group for four reasons: it associates strongly with imidazole groups, its coordination to imidazole groups can be followed spectrophotometrically, it is commercially available, and it is well explored in the literature, notably by Sanders⁵ and Groves.⁶ The results presented in this paper are summarized in Table 2.

Organization of This Paper. The results section is organized into three parts. The first describes syntheses of the molecules and aggregates; the second discusses the association of *n*-butylimidazole (bu-Im) with ZnTPP; the third summarizes the characterization of aggregates **1–4**, organized by method of characterization so that comparisons of **1** and **3** with **2** and **4** can be made efficiently.

Results and Discussion

Synthesis. Scheme 1 summarizes the syntheses of the components of **1–4**. We prepared aggregate **1** by mixing the components in CD₂Cl₂ followed by sonication and brief heating at reflux. Synthesis of **3** was accomplished

by adding one drop of methanol to a suspension of the components in CH₂Cl₂, evaporating the resulting homogeneous solution to dryness, and redissolving the residue in CD₂Cl₂. To prepare **2** and **4**, the appropriate amount (3 or 6 equiv) of ZnTPP was added to the solution of aggregates **1** and **3**.

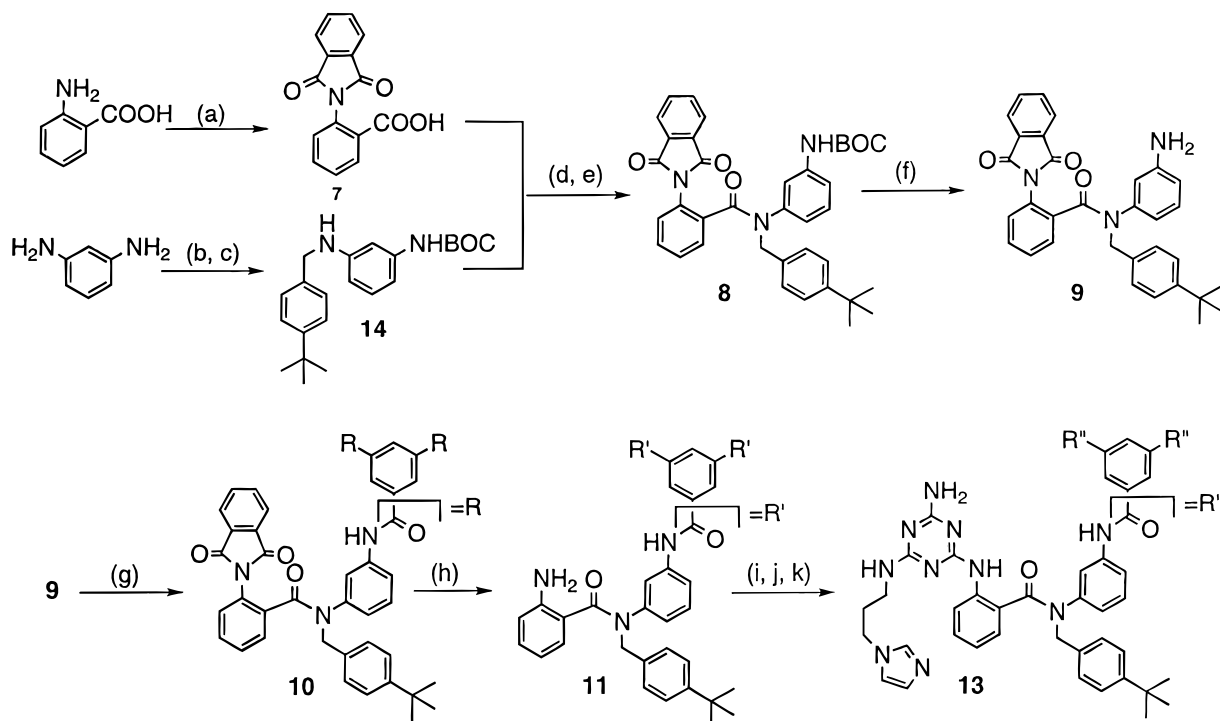
Bu-Im•ZnTPP. The interaction of metal porphyrins with imidazole groups is well documented.⁴ In our system, visual inspection, UV/vis spectroscopy, and ¹H NMR spectroscopy suggest that ZnTPP•bu-Im forms rapidly on mixing ZnTPP and bu-Im.

Visual Inspection and UV/vis Spectroscopy. Upon addition of bu-Im to a solution of ZnTPP, the color of the solution changes from violet to blue. No color change occurs when derivatives of CA or M lacking an imidazole group are added; this observation suggests that the interaction between imidazole and ZnTPP is specific. UV/vis spectroscopy confirms these visual observations. Figure 1 shows the UV/vis spectral titration for a fixed concentration of ZnTPP (10 μM in CH₂Cl₂) while changing the concentration of bu-Im (0–60 μM). The Soret band of ZnTPP shifts from 418 to 428 nm. Nonlinear least-squares analysis of these data (monitoring at 418 nm) yields the binding constant for bu-Im with ZnTPP; *K*_a = 1.8 × 10⁵ M⁻¹ s⁻¹. In addition to the changes in the Soret band, the Q-band of ZnTPP at 547 nm weakens and new bands appear at 565 and 603 nm upon addition of bu-Im. These changes in the UV/vis spectrum do not fit to a simple 1:1 binding event. Changes in the position and intensity of the Soret band will, therefore, be most useful in monitoring the aggregation events on the periphery of the CA•M rosette.

¹H NMR Spectroscopy. The ¹H NMR spectrum at 240 K suggests that ZnTPP forms a 1:1 aggregate with bu-Im. On mixing solutions of ZnTPP and bu-Im, all of

(5) Anderson, S.; Anderson, H. L.; Sanders, J. K. M. *Acc. Chem. Res.* **1993**, *26*, 469 and references therein.

(6) Lahiri, J.; Fate, G. D.; Ungashe, S. B.; Groves, J. T. *J. Am. Chem. Soc.* **1996**, *118*, 2347 and references therein.

Scheme 1. Synthesis of Hub(M^{Im})₃^a

^a Key: (a) phthaloyl dichloride, triethylamine; (b) (*t*-BuOCO)₂O, THF; (c) *tert*-butylbenzyl bromide, diisopropylethylamine (DIPEA); (d) 7 and SOCl₂, then (e) DIPEA and **14**; (f) trifluoroacetic acid/CH₂Cl₂; (g) 1,3,5-benzenetricarbonyl chloride, DIPEA, THF; (h) H₂NNH₂ in MeOH; (i) cyanuric chloride, DIPEA, THF; (j) NH₃(g); (k) aminopropylimidazole, DIPEA, dioxane.

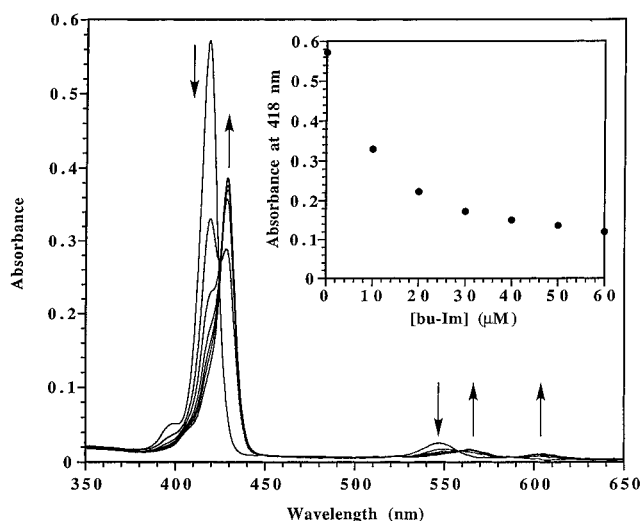


Figure 1. UV/vis spectral titration of ZnTPP (10 μ M in CH₂Cl₂) with bu-Im (0–60 μ M). The arrows indicate the increase or decrease in absorbance of the indicated band as bu-Im is added. The inset shows a plot of the concentration of bu-Im versus absorbance at 418 nm used to determine the binding constant.

the aliphatic resonances of bu-Im shift upfield. The pyrrole protons of ZnTPP shift from 9.0 to 8.9 ppm. At room temperature, the aromatic resonances of the imidazole broaden into the base line; they appear dramatically shifted upfield at low temperature. No lines corresponding to free bu-Im appear until the ratio of bu-Im:ZnTPP becomes greater than 1; we infer that only a 1:1 complex, ZnTPP·bu-Im, is formed. This observation suggests that the off-rate for the ZnTPP·bu-Im interaction is slow on the NMR time scale.

Characterization of 1–4. Proof of structure for **1–4** comes from four primary sources: stoichiometry, as

shown by titrations; structure, from ¹H NMR spectroscopy; molecular weights, as established using ESI-MS; and stabilities, inferred from GPC. The incorporation of a ZnTPP·imidazole interaction allows color changes to be monitored either by UV/vis spectroscopy or by eye.

Stoichiometry. To establish the ratio of hub(M^{Im})₃ to CA (or bisCA), we slowly added the CA component into a solution of CD₂Cl₂ containing hub(M^{Im})₃. We monitored this titration by ¹H NMR spectroscopy and by visual inspection. Both techniques indicate the stoichiometries shown in Table 2. As the CA component is added, the ¹H NMR spectrum of a solution of hub(M^{Im})₃ in CD₂Cl₂ goes from broad and featureless—except for solvent and a broad *t*-Bu resonance—to sharp lines. The intensities of these lines increased until 3 equiv of CA had been added. Additional CA did not affect the spectrum: the CA was insoluble and was visible as suspended powder.

¹H NMR Spectroscopy. Strong spectral correlations involving three different aspects of the ¹H NMR spectra of **1–4** lead us to the conclusion that **1** and **2** are structurally analogous to **5** and that **3** and **4** are analogous to **6**.

Line Width. The spectrum of hub(M^{Im})₃ in the absence of CA is featureless: a rolling base line showing a line for solvent and a broad resonance corresponding to the *tert*-butyl groups. Sharp lines—obtained upon addition of CA—establish that discrete, nonrandom species (**1** and **3**) exist in solution. Similar behavior had been observed previously for aggregates **5** and **6**. Addition of ZnTPP to solutions of **1** and **3** generates **2** and **4**. The ¹H NMR spectra of these aggregates are sharp and indicate that well-defined aggregates exist in solution.

Hydrogen-bonded Protons. Sharp resonances between 16 and 13 ppm are due to the hydrogen-bonded imide protons of CA. In DMSO-*d*₆ these protons appear at 9.5 ppm. The number of lines corresponding to

hydrogen-bonded protons establishes the symmetry of the aggregate: for example, two lines are observed for the C_3 -symmetric isomer of **5**; six lines are observed for its C_1 -symmetric isomer. The imide regions of the ^1H NMR spectra for **1–4** are shown in Table 2. Aggregates **1** and **2**, just like **5**, show only two resonances in the imide region of the ^1H NMR spectrum. This spectrum is consistent, in each case, with the presence of a single aggregate of C_3 -symmetry. Aggregate **3**, however, shows 12 resonances in the imide region of its ^1H NMR spectrum; two of high intensity and 10 (two more are not readily identified as a result of coincidental overlap) of lower intensity. This observation can be rationalized by the presence of two aggregates, one of D_3 symmetry, the other C_1 symmetric.³ The spectra collected previously for **6** showed similar patterns. In contrast, the imide region of the ^1H NMR spectrum of **4** shows only two resonances, suggesting the presence of a single aggregate of D_3 symmetry.

Diastereotopic Protons. Many methylene groups should—and do—appear as sets of diastereotopic protons. Each diastereotopic proton is easily identified as a doublet, and several are of markedly different chemical shift as a result of the relative proximity of the aromatic rings of the trismelamine. In particular, the methylene group of the *tert*-butyl benzyl substituent is diagnostically valuable. In aggregates **1–4**, these protons resonate at around 4 and 5.5 ppm; the ~ 1.5 ppm separation indicates a well-defined structure and can be explained by the presence of a nearby aromatic ring.

Assignment. The line widths of the ^1H NMR spectra, the intensity, multiplicity and location of the resonances for the imide protons, and the presence and location of diagnostic sets of diastereotopic protons for aggregates **1–4** and **5–6** are strikingly similar. The main differences are due to the presence of ZnTPP in aggregates **3** and **4**, which leads to slight broadening of resonances and a pronounced upfield shift in many resonances on the periphery of the aggregate. The strong structural similarity of the components of **1–4** and **5–6**, when coupled with these strong NMR correlations among these aggregates, fully justifies the following structural assignments. The number and intensity of resonances in the imide region of the ^1H NMR spectrum for **1** and **2** are consistent with a single aggregate existing as a pair of enantiomers with C_3 symmetry.⁸ Two isomers are observed for **3**, whereas a single isomer is observed for **4**. Using **5** and **6** as model compounds, the structural assignment of these aggregates is straightforward. Aggregate **3** exists as two isomeric forms: the major isomer has D_3 symmetry; the minor is C_1 symmetric. Aggregate **4**, however, exists as a single species in solution; we assign D_3 symmetry to this aggregate.

ESI-MS. The spectrograms for **1** and **3** are very simple: only one line ($1\cdot\text{Cl}^-$ or $3\cdot 2\text{Cl}^-$) is observed over

a range of ionization conditions: only under high voltages ($V > 90$) and temperatures ($T > 60$ °C) was a small line corresponding to free hub($\text{M}^{\text{im}}\text{)}_3$ observed.¹⁰ A single line does not prove unambiguously that **1** and **3** are the only stable species *in solution*, since ESI-MS measures the m/z ratio for aggregates in the gas phase. These results do, however, agree with those from ^1H NMR spectroscopy and reinforce the inference that a single species (**1** and **3**) is present.

The mass spectra of **2** and **4** contain more lines than those of **1** and **3**. Intense lines are observed at masses corresponding to $2\cdot 2\text{Cl}^-$ and $4\cdot 3\text{Cl}^-$, but additional lines complicate the spectrogram. Some of these remaining lines correspond to the loss of ZnTPP (Table 2). The loss of ZnTPP is not surprising; even though the imidazole·Zn chelate interaction is stronger than a single hydrogen bond it is probably the easiest bond to break in the entire assembly since the hydrogen bonds of the rosette act in concert. Observation of these aggregates, in fact, would probably not be possible except for the fact that we are using Ph_4PCl as the charge carrier.¹⁰ Other lines—most less than 10% intensity—are difficult to assign and may result from aggregation of matrix (Ph_4Cl) with itself or molecules of aggregate.

Gel Permeation Chromatography.¹¹ GPC is a size exclusion technique. The pores of the stationary phase readily allow small molecules to enter while excluding larger molecules. The direct result is that smaller molecules take longer to pass through the column than larger molecules. The stability of hydrogen-bonded aggregates based on the CA·M motif is reflected in the extent of tailing of the peaks.¹¹ Stable aggregates elute from the column as sharp peaks. Tailing results from the dissociation of the aggregates into soluble, slower moving components. That is, while we expect that **1** should elute similarly to **5** based on the similarity of their structures, the broad peak (lacking a well-defined leading edge) observed in the trace (Table 2) suggests that **1** is unstable under the conditions of GPC. The traces suggest that **5** and **2** are of comparable stability and that both are more stable than **1**. Similarly, **6** and **4** are more stable than **3**. The traces for **2** and **4** show two peaks: one peak coelutes with ZnTPP. It is unclear whether the

(9) The shifts and broadening observed in the ^1H NMR spectra make the upfield region of the spectra difficult to assign. We can easily discern, however, that C_3 symmetry of the aggregate is maintained and that the structures of these imidazole-containing aggregates are very similar to those of **5** and **6**. Assignment of all the resonances—especially those corresponding to the chelated imidazole group—are, therefore, tentative. The imide region of the spectrum, however, is diagnostic of the symmetry and number of aggregates present in solution.

(10) (a) Cheng, X. H.; Gao, Q. Y.; Smith, R. D.; Simanek, E. E.; Mammen, M.; Whitesides, G. M. *J. Org. Chem.* **1996**, *61*, 2204–2206. (b) Cheng, X. H.; Gao, Q. Y.; Smith, R. D.; Simanek, E. E.; Mammen, M.; Whitesides, G. M. *Rapid Commun. Mass Spec.* **1995**, *9*, 312–316. (c) Cheng, X. H.; Chen, R. D.; Bruce, J. E.; Schwartz, B. L.; Anderson, G. A.; Hofstadler, S. A.; Gale, D. C.; Smith, R. D.; Gao, J. M.; Sigal, G. B.; Mammen, M.; Whitesides, G. M. *J. Am. Chem. Soc.* **1995**, *117*, 8859–8860. The observation of zinc porphyrin-imidazole assemblies in the ESI-MS spectrogram was possible in this case due to the special conditions employed. Such aggregates are expected to be difficult to observe using ionization from protic solvents since the protonation of the most basic site—the imidazole—leads to destruction of the aggregate. The ESI-MS experiments described here use Ph_4PCl as a charge carrier; we are able to observe $[\text{M} + \text{Cl}^-]$ in the negative-ion mode. The use of CH_2Cl_2 as solvent may also limit the extent to which protonation occurs. The significant number of extra lines remains a challenge to interpret. Further investigation of other alternatives to H^+ as the ion source, including Ph_4PCl , may lead to spectra with fewer ambiguous lines.

(11) For a more complete description of our use of GPC see ref 1 or: Mathias, J. P.; Seto, C. T.; Simanek, E. E.; Whitesides, G. M. *J. Am. Chem. Soc.* **1994**, *116*, 1725.

(7) Melamines and derivatives of CA containing covalently tethered porphyrins have been reported by a number of groups. See: Ichihara, K.; Naruta, Y. *Chem. Lett.* **1995**, 631. Drain, C. M.; Russell, K. C.; Lehn, J.-M. *Chem. Commun.* **1996**, 337. Drain, C. M.; Fischer, R.; Nolen, E.; Lehn, J.-M. *J. Chem. Soc. Chem. Commun.* **1993**, 243 and references therein.

(8) All three arms twist in the same direction with respect to both the core benzene-1,3,5-tricarbonyl and the melamine groups. A second isomer with C_1 symmetry has been observed in related structures and is generated conceptually by rotation of the melamine about the indicated spoke. The loss of C_3 symmetry leads to a 3-fold increase in the number of lines in the imide region of the ^1H NMR spectrum. These isomers have been investigated in: Simanek, E. E.; Wazeer, M. I. M.; Mathias, J. P.; Whitesides, G. M. *J. Org. Chem.* **1994**, *59*, 4904.

faster eluting peak corresponds to intact **2** or a species containing less than three ZnTPP. The position of the peak in the GPC trace of **2** when compared with the position of **5** suggests that the species that elutes is larger than **5**. That is, the species that elutes contains at least one porphyrin. A hint of color in the eluent is consistent with this belief.

Ultraviolet and Visible (UV/vis) Spectroscopy. The changes in the UV/vis spectrum that occur on addition of bu-Im to a solution of ZnTPP in CH₂Cl₂ are diagnostic for formation of a Zn-imidazole interaction. We have, accordingly, used this spectroscopic marker to follow the association of ZnTPP with self-assembled aggregates **1** and **3**. The experimental design was crucial; the extremely high extinction coefficient of the Soret band for ZnTPP gives an upper limit for ZnTPP concentration of 100 μ M. Furthermore, a lower concentration for aggregates **1** and **3** was set at 10 μ M, since aggregates based on the CA·M lattice are stable at this concentration.² On the basis of these considerations, we performed Job plots to determine the stoichiometry of the interaction of **1** and **3** with ZnTPP.

The results of Job titrations of **1** and **3** (constant total concentration [**1**] + [**3**] = 100 μ M in CH₂Cl₂) are shown in Figure 2a. As the concentrations of **1** and ZnTPP are changed, the relative intensities of the Soret bands at 418 and 427 nm are affected; these changes allow quantitation of the number of ZnTPP molecules that bind to **1** at this concentration. The inset (Figure 2a) shows a Job plot of the mole fraction of ZnTPP (defined as [ZnTPP]/([ZnTPP] + [**1**])) versus absorbance at 427 nm. This plot shows a maximum when the mole fraction of ZnTPP is between a ratio of 1:ZnTPP of 1:2 and 1:3. This result, when combined with the results of the ¹H NMR experiments described above, is strong evidence for the formation of the 1:3 aggregate **2**.

Similar UV/vis Job experiments were performed using the bisosette **3** and ZnTPP. Figure 2b shows the UV/vis spectra recorded for different mole fractions of **3** and ZnTPP at a constant total concentration of 100 μ M. Once again, the intensities of the Soret bands of free ZnTPP and chelated ZnTPP change as a function of mole fraction. The inset (Figure 2b) shows a plot of the mole fraction of ZnTPP versus absorbance at 427 nm. This plot shows a maximum at a mole fraction of ZnTPP of 0.80. This corresponds to a 1:4 molar ratio of **3**:ZnTPP, suggesting that aggregate **4** does not contain a full six ZnTPP molecules organized around its periphery. This result is not inconsistent with the results of ¹H NMR experiments described above for the following reasons: (1) the error in Job plots can be substantial, especially when dealing with higher order complexes, and (2) this experiment was performed at a total concentration of 100 μ M, far below the 5 mM concentration employed for ¹H NMR. It is plausible that the fifth and sixth equivalent of ZnTPP require higher concentrations for complex formation as a result of unfavorable steric interactions.

Imidazole Groups Not Involved in Chelation Decrease the Stability of Hydrogen-Bonded Aggregates. GPC reveals that **5** is more stable than **1** and **6** is more stable than **3**. Adding ZnTPP—to form **2** and **4**—appears to increase the stability of the aggregates. That is, these data suggest that the imidazole groups destabilize hydrogen-bonded aggregates when they are not coordinated to a metal atom. The traces for **2** and **4** have sharp leading edges and are shaped like the traces for **5** and **6**. A trace of tris(2-aminoimidazole) and ZnTPP is

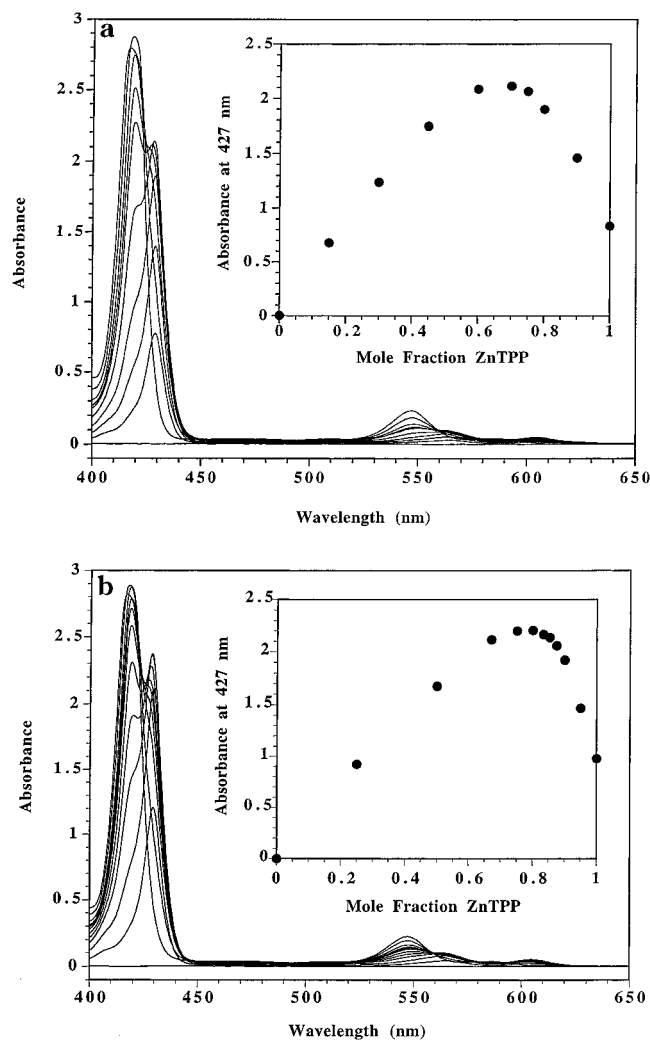


Figure 2. (a) UV/vis spectral titration at a fixed total concentration (100 μ M) of ZnTPP and **1** in CH₂Cl₂. The inset shows a Job plot of the mole fraction of ZnTPP versus absorbance at 427 nm. (b) UV/vis spectral titration at a fixed total concentration (100 μ M) of ZnTPP and **3** in CH₂Cl₂. The inset shows a Job plot of the mole fraction of ZnTPP versus absorbance at 427 nm.

indistinguishable from a trace of ZnTPP. These trends in stability are born out in competition experiments described below.

We envision that the destabilizing effect of the imidazole group results from their ability to form hydrogen bonds with both the NH groups of melamine and isocyanuric acid groups. For the aggregate to form, the hydrogen bonds formed with imidazole groups must be broken at an enthalpic cost. As a result, the net enthalpy of formation of the hydrogen bonds between isocyanuric acid and melamine is decreased and the overall enthalpy of formation of the aggregate is also decreased.

Mixing hub(M)₃ and hub(M^{Im})₃ with an Amount of CA Less than the 1:3 Stoichiometry Required for the Formation of Aggregates Shows that **5 Is More Stable than **1**.** Adding hub(M)₃ to a solution of **1** leads to the rapid formation of **5** and free hub(M^{Im})₃ in a ratio that is greater than 10:1. This result is consistent with the results obtained from GPC: **5** is more stable than **1**. Unfortunately, the spectrum of this mixture is complicated by the presence of other hydrogen-bonding species. These species exist in small—but significant—amounts and prevent further analysis of the relative stability of

5 and **1**. These species do serve as a warning: hydrogen bonds (on melamines) left unsatisfied can promote the formation of undesired aggregates.

Addition of ZnTPP to an equimolar solution of **5** and hub(M^{lm})₃ leads to the formation of **2**. At 3 equiv of ZnTPP—in terms of hub(M^{lm})₃—the resulting solution is a 3:2 mixture of **5:2**. Additional resonances (existing in <20%) correspond to other structurally undefined, hydrogen-bonded aggregates.

The similarity in the stabilities of **2** and **5** is intuitively reasonable. The change from a *tert*-butyl group to an imidazole group on the periphery of a hydrogen-bonded aggregate should only affect the stability of the aggregate by competing for hydrogen bonds. Upon formation of a zinc-imidazole interaction, the competition for hydrogen bonds does not occur and the resulting aggregate—barring unfavorable steric interactions between the chelating group and the original scaffold—should be comparable in stability to the *tert*-butyl analogue.

Influence of ZnTPP on Isomers of 3 and 4. The ¹H NMR spectrum of **3**, and in particular the presence of two plus 12 resonances in the imide region, establishes that **3** exists as a mixture of two isomeric aggregates of C₃ and C₁-symmetry. Similar behavior for **5** had been observed previously. Computational results³ have been used to rationalize the observed distribution of isomers; these results are based on the assumption that eclipsing interactions between rosettes is unfavorable. When 6 equiv of ZnTPP is added to **3** to generate **4**, the imide region of the ¹H NMR is simplified; the spectrum now contains only two resonances for the hydrogen-bonded imide protons. This observation suggests that as the sterically bulky ZnTPP coordinates on the periphery of these aggregates, the preference for the isomer that allows the fewest unfavorable steric interactions is increased. The resulting aggregate consists of only a single isomer, probably of D₃ symmetry.

Conclusions

This work establishes that imidazole groups are compatible with hydrogen-bonded aggregates based on the CA·M lattice. Aggregates containing imidazole groups are less stable than their *tert*-butyl analogues. We hypothesize that this difference in stability reflects the capacity of imidazole groups to compete for hydrogen bonds. Addition of ZnTPP yields aggregates of the expected 1:1 stoichiometry of imidazole:ZnTPP. These aggregates are more stable than those presenting free imidazole groups and are of comparable stability to the *tert*-butyl analogues.

The incorporation of zinc-imidazole interactions in aggregates based on CA·M is our first attempt at *hierarchical* self-assembly—the noncovalent synthesis of many particles into a discrete aggregate using multiple types of interactions. The important conclusion is that the stability of the aggregates that we have reported—and presumably of the family of aggregates—is not affected by the presence of imidazole groups when ZnTPP coordinates to the imidazole groups.

Experimental Section

General Methods. Starting materials were obtained from commercial sources (Aldrich and Fluka) and were used without further purification. Compound **14** was available from previous studies. NMR spectra were collected on a Bruker AM-400 equipped with a Wescan-1000 temperature monitoring

apparatus. Unless otherwise noted, all aggregation experiments were performed at a concentration of 5 mM. GPC was performed with a Waters 600E HPLC system with a Waters Ultrastaygel 10 column employing a flow rate of 1 mL min⁻¹ with a 10 μL injection volume, with a Waters 484 detector at 254 nm. UV/vis spectra were acquired on a Hitachi U-3210 instrument as solutions in CH₂Cl₂; for porphyrin-containing aggregates, a 1-mm path length cell was employed.

2-[(1,3-Dihydro-1,3-dioxo-2H-isoindol-2-yl)benzoic Acid (7). The title compound was prepared by the reported method:² ¹H NMR (400 MHz, DMSO-*d*₆) δ 13.2 (bs, 1H), 8.11 (d, *J* = 5.1 Hz, 1H), 7.98 (m, 2H), 7.92 (m, 2H), 7.76 (t, *J* = 5.1 Hz, 1H), 7.62 (t, *J* = 4.3 Hz, 1H), 7.54 (d, *J* = 4.3 Hz, 1H); ¹³C NMR (100 MHz, DMSO-*d*₆) δ 167.12, 166.09, 134.80, 132.97, 131.75, 131.48, 131.02, 130.66, 130.13, 129.25, 123.50; HRMS-FAB (M+Na⁺) calcd for C₁₅H₉NO₃Na 290.0249, found 290.0239.

3-[[2-(1,3-Dihydro-1,3-dioxo-2H-isoindol-2-yl)benzoyl]][4-(1,1-dimethylethyl)phenyl]methyl]aminol]phenyl]carbamic Acid 1,1-Dimethylethyl ester (8). The title compound was prepared by the reported method:² ¹H NMR (400 MHz, DMSO-*d*₆) δ 9.39 (s, 1H), 8.02 (m, 2H), 7.95 (m, 2H), 7.59 (s, 1H), 7.48 (m, 2H), 7.25–7.05 (m, 5H), 7.14 (m, 2H), 6.93 (bs, 2H), 4.90 (bs, 2H), 1.45 (s, 9H), 1.21 (s, 9H); ¹³C NMR (100 MHz, DMSO-*d*₆) δ 166.97, 166.41, 152.50, 149.04, 142.98, 140.21, 134.79, 133.94, 133.06, 131.56, 130.13, 130.74, 130.09, 129.48, 128.57, 127.80, 126.74, 124.84, 123.47, 121.91, 116.36, 52.24, 31.06, 28.05, 25.06; HRMS-FAB (M + Na⁺) calcd for C₃₇H₃₇N₃O₅Na 626.2631, found 626.2635.

3-[[2-(1,3-Dihydro-1,3-dioxo-2H-isoindol-2-yl)benzoyl]][4-(1,1-dimethylethyl)phenyl]methyl]aminol]aniline (9). A solution of **8** (4.5 g, 7.5 mmol) in CH₂Cl₂ (30 mL) was cooled in an ice bath, and trifluoroacetic acid (1 mL) was added. The ice bath was removed, and the reaction was stirred at rt overnight. TLC (19:1 CH₂Cl₂:MeOH) revealed a quantitative conversion to **4**. The organic phase was washed with saturated aqueous NaHCO₃ (2 × 30 mL) and H₂O (30 mL) and dried over Na₂SO₄. Concentration afforded **4** (3.8 g, 100%) as an off-white solid: ¹H NMR (400 MHz, DMSO-*d*₆) δ 8.03 (m, 2H), 7.95 (m, 2H), 7.50 (bs, 2H), 7.24–7.07 (m, 7H), 6.88 (d, *J* = 5 Hz, 1H), 6.36 (bs, 2H), 4.95 (s, 2H), 1.22 (s, 9H); ¹³C NMR (100 MHz, DMSO-*d*₆) δ 167.17, 149.19, 143.78, 134.91, 133.88, 132.83, 131.60, 131.16, 130.32, 129.65, 129.39, 128.87, 128.16, 127.79, 126.84, 126.75, 125.28, 124.93, 123.56, 122.68, 117.93, 115.50, 117.06, 52.33, 34.07, 31.08; HRMS-FAB (M + Na⁺) calcd for C₃₂H₂₉N₃O₃Na 526.2107, obsd 526.2064.

***N,N,N'*-Tris[3-[[2-(1,3-Dihydro-1,3-dioxo-2H-isoindol-2-yl)benzoyl]][4-(1,1-dimethylethyl)phenyl]methyl]aminol]phenyl]-1,3,5-benzenetricarboxamide (10).** A solution of **4** (1.4 g, 2.8 mmol) in CH₂Cl₂ (10 mL) was added dropwise to an ice-cold solution of 1,3,5-benzenetricarbonyl chloride (245 mg, 0.9 mmol) and diisopropylethylamine (DIPEA) (180 mg, 0.25 mL, 14 mmol) in CH₂Cl₂ (200 mL). The ice bath was removed, and the reaction mixture was stirred overnight. Following evaporation of the reaction mixture, EtOAc (100 mL) was added to the residue, and the organic layer was washed with H₂O (2 × 50 mL), dried over MgSO₄, and evaporated onto SiO₂. Chromatography (9:1 CH₂Cl₂:MeOH) afforded **5** as a white solid (1.3 g, 85%): ¹H NMR (400 MHz, DMSO-*d*₆) δ 10.68 (s, 1H), 8.70 (s, 1H), 8.03 (m, 3H), 7.92 (m, 2H), 7.6 (d, 1H, 4.8 Hz), 7.49 (bs, 2H), 7.24 (m, 4H), 7.14 (bs, 4H), 4.99 (bs, 2H), 1.22 (s, 9H); ¹³C NMR (100 MHz, DMSO-*d*₆) δ 167.04, 166.54, 164.43, 149.15, 143.00, 139.56, 135.27, 134.84, 133.94, 131.59, 130.92, 130.27, 130.17, 129.86, 129.60, 128.79, 127.85, 126.77, 133.03, 124.94, 123.82, 123.53, 118.64, 117.85, 52.34, 34.07, 31.08; HRMS-FAB (M + Na⁺) calcd for C₁₀₅H₈₇N₉O₁₂Na 1686, found 1686; MS ion profile calcd (M + Na⁺) *m/z* (relative intensity) 1689 (82), 1690 (100), 1691 (62), 1692 (27), 1693 (9), found 1689 (88), 1690 (100), 1691 (64), 1692 (30), 1693 (11).

***N,N,N'*-Tris[3-[(2-aminobenzoyl)][4-(1,1-dimethylethyl)phenyl]methyl]aminol]phenyl]-1,3,5-benzenetricarboxamide (11).** A solution of **5** (1.2 g, 0.7 mmol) in MeOH (50 mL) was cooled in an ice bath. Hydrazine (61 mg, 2.2 mmol) was added. The ice bath was removed, and the reaction mixture was heated at reflux for 6 h. Following evaporation of the reaction mixture, the residue was resuspended in EtOAc

(100 mL), washed with H₂O (3 × 50 mL), dried over Na₂SO₄, and evaporated onto SiO₂. Chromatography (19:1 CH₂Cl₂:MeOH) afforded **11** as a white solid (0.9 g, 90%): ¹H NMR (400 MHz, DMSO-*d*₆) δ 10.54 (s, 1H), 8.61 (s, 1H), 7.74 (s, 1H), 7.55 (d, 1H, *J* = 4.6 Hz), 7.33 (d, 2H, *J* = 5.1 Hz), 7.26 (d, 2H, *J* = 5.1 Hz), 7.14 (t, 1H, *J* = 4.8 Hz), 6.94 (t, 1H, *J* = 4.5 Hz), 6.84 (d, 1H, *J* = 4.8 Hz), 6.74 (d, 1H, *J* = 4.5 Hz), 6.65 (d, 1H, *J* = 5.1 Hz), 6.27 (t, 1H, *J* = 4.6 Hz), 5.50 (bs, 2H), 5.05 (s, 2H), 1.24 (s, 9H); ¹³C NMR (100 MHz, DMSO-*d*₆) δ 170.24, 167.03, 164.33, 149.28, 147.60, 143.79, 139.37, 135.16, 134.60, 134.29, 130.21, 129.78, 128.89, 128.81, 127.14, 125.08, 124.97, 124.96, 122.77, 122.72, 118.69, 118.09, 118.01, 115.78, 114.83, 52.46, 34.11, 31.09; HRMS-FAB (*M* + Na⁺) calcd for C₈₁H₈₂N₉O₆-Na 1290, found 1290; MS ion profile calcd (*M* + Na⁺) *m/z* (relative intensity) 1296 (19), 1297 (23), 1298 (100), 1299 (89), 1300 (43), 1301 (16); found 1296 (18), 1297 (23), 1298 (100), 1299 (88), 1300 (43), 1301 (16).

Trichloride 12. Trianiline **11** (400 mg, 0.3 mmol) was dissolved in THF (3 mL) and then added dropwise to an ice-cold solution of cyanuric chloride (345 mg, 1.9 mmol) and DIPEA (1.5 g, 2 mL, 120 mmol) in THF (50 mL). The reaction was allowed warm to room temperature over 1 h, at which time NH₃(g) was bubbled through the solution for 15 min and then stirred overnight. The reaction mixture was evaporated to dryness and partitioned between aqueous 0.1 N NaOH (50 mL) and EtOAc (30 mL). The aqueous layer was washed with ethyl acetate (2×), and the organic layers were combined and dried over Na₂SO₄. The crude product obtained after filtration and evaporation was used in the next reaction without further purification.

***N,N,N'*-Tris[3-[[2-[[4-amino-6-(3-imidazolyl-*N*-propylamino)-1,3,5-triazine-2-yl]amino]benzoyl]][4-(1,1-dimethylethyl)phenyl]methyl]amino]phenyl]-1,3,5-benzenetricarboxamide, Hub(M^{Im})₃, (**13**).** The crude trichloride **12** was dissolved in dioxane (10 mL), and aminopropylimidazole (1.0 g, 1.0 mL, 8 mmol) was added. After heating at reflux overnight, the reaction mixture was cooled to rt and

concentrated. The reaction mixture was partitioned between aqueous 0.1 N NaOH and EtOAc. The aqueous layer was extracted with EtOAc (6 × 30 mL), the combined organic layer was dried over Na₂SO₄, and the crude material was absorbed onto silica gel. Chromatography (90:10:1 CH₂Cl₂:MeOH:NH₄-OH) gave **13** (375 mg, 65%) as an off-white solid: ¹H NMR (400 MHz, DMSO-*d*₆) δ 10.56 (s, 1H), 8.59 (s, 2H), 7.75 (s, 1H), 7.58 (m, 2H), 7.32 (d, *J* = 5.1 Hz, 2H), 7.26 (m, 3H), 7.14 (m, 2H), 7.05 (bs, 1H), 6.94 (t, *J* = 4.5 Hz, 1H), 6.82 (m, 1H), 6.70–6.40 (m, 3H), 5.08 (bs, 2H), 3.96 (bs, 2H), 3.17 (bs, 2H), 1.90 (bs, 2H), 1.22 (s, 9H); ¹³C NMR (100 MHz, DMSO-*d*₆) δ 143.84, 140.15, 139.78, 135.69, 134.70, 128.86, 127.60, 125.68, 119.72, 118.86, 118.54, 52.85, 43.71, 34.07, 30.99, 30.65; HRMS-FAB (*M* + Na⁺) calcd for C₁₀₈H₁₁₅N₃₀O₆Na 1950, found 1950; MS ion profile calcd (*M* + Na⁺) *m/z* (relative intensity) 1949 (75), 1950 (100), 1951 (66), 1952 (30); found 1949 (85), 1950 (100), 1951 (72), 1952 (42).

Acknowledgment. E.E.S. was an Eli Lilly Predoc-toral Fellow (1995). L.I. thanks the NIH for a postdoc-toral fellowship and Dr. Joydeep Lahiri for many helpful discussions. The spectrometer facility is supported by NIH Grant No. 1-S10-RR04870-01 and NSF Grant No. CHE-88-14019. This work was supported by the NSF (Grant No. CHE-91-22331). Mass spectrometry was performed by Dr. Andrew Tyler. The Harvard Mass Spectrometry Facility is supported by NIH RR 08458.

Supporting Information Available: ¹H NMR spectra and ESI-MS spectrograms for 1–4 (8 pages). This material is contained in libraries on microfiche, immediately follows this article in the microfilm version of the journal, and can be ordered from the ACS; see any current masthead page for ordering information.

JO9615458